Nonlinear robust control of tail-sitter aircrafts in flight mode transitions

Zhaoying Li[a], Lixin Zhang[a], Hao Liu[a,*], Zongyu Zuo[b], Cunjia Liu[c]

[a]*School of Astronautics, Beihang University, Beijing 100191, P.R. China.*
[b]*The Seventh Research Division, Beihang University, Beijing 100191, P.R. China.*
[c]*Department of Aeronautical and Automotive Engineering, Loughborough University, Leicestershire, England LE11 3TU, United Kingdom*

Abstract

In this paper, a nonlinear robust controller is proposed to deal with the flight mode transition control problem of tail-sitter aircrafts. During the mode transitions, the control problem is challenging due to the high nonlinearities and strong couplings. The tail-sitter aircraft model can be considered as a nominal part with uncertainties including nonlinear terms, parametric uncertainties, and external disturbances. The proposed controller consists of a nominal H_∞ controller and a nonlinear disturbance observer. The nominal H_∞ controller based on the nominal model is designed to achieve the desired trajectory tracking performance. The uncertainties are regarded as equivalent disturbances to restrain their influences by the nonlinear disturbance observer. Theoretical analysis and simulation results are given to show advantages of the proposed control method, compared with the standard H_∞ control approach.

Keywords: tail-sitter aircraft, flight mode transition, unmanned aerial vehicle, robust control, nonlinear system

1. Introduction

In recent years, the unmanned aerial vehicles (UAVs) have attracted much attention because of their various applications (see, e.g., [1, 2, 3, 4, 5]). Tail-sitter aircrafts are a new type of UAVs, which can vertical take off and land (VTOL) on their tails, and fly forward with high speeds and heavy loads. Due to these advantages, the tail-sitter aircrafts have drawn much attention and have various applications in civil and military fields, as shown in [1]. The flight mode transition of tail-sitter aircraft is a process that the aircraft flies forward from hovering, or vice versa [3, 6]. During the flights of the tail-sitter aircraft, including flying forward, hovering, mode transition, take-off and landing, multiple challenges exist such as nonlinearities and uncertainties involved in the vehicle dynamics for the flight control method design, especially in the flight mode transitions [7]. The tail-sitter aircraft is the

*Corresponding author.
Email addresses: lizhaoying@buaa.edu.cn (Zhaoying Li), buaazlx@buaa.edu.cn (Lixin Zhang), liuhao13@buaa.edu.cn (Hao Liu), zzybobby@buaa.edu.cn (Zongyu Zuo), c.liu5@lboro.ac.uk (Cunjia Liu)

combination of the fixed-wing aircraft and the rotorcraft, which has the both characteristics of the fixed-wing aircraft and rotorcraft. It can vertically taking off and hover like rotorcraft while cruise with high flight speed and long flight time and can accomplish multiple complex tasks, which is hard for either fixed-wing aircraft or rotorcraft. The main difficulty of control is about that the flight mode transition due to the large maneuver, the serious nonlinearity and influences of the uncertainty. In the mode transition, the fuselage is tilted and the wings are kept at a given small angle of attack. However, it is difficult to analyze the aerodynamics of the tilting fuselage during the mode transition, and moreover, the tilting structure is difficult to control. Several design methodologies of tail-sitter aircrafts are introduced in [8, 9].

In recent years, developments of the tail-sitters have made significant progress. Many efforts have been applied to deal with the flight control problem of the tail-sitter aircrafts. As shown in [10]-[11], a twin helicopter rotor tail sitter aircrafts are presented. A model of an agile tail-sitter aircraft was presented in [12], which could operate as a helicopter as well as have the capable of transition to fixed-wing flight. A novel hybrid UAV called U-Lion was introduced in [13], which had autonomous VTOL and cruise flying capabilities. As shown in [14], an accurate and robust altitude control method was presented for VTOL aircrafts equipped with turbine engines in order to achieve the quasi-stationary flight. To support navigation and control research for indoor micro air vehicles, a four wing tail-sitter type rotorcraft micro air vehicle was developed in [15]. Based on aerodynamics characteristics of a fixed-wing micro air vehicle, the influence of a propeller slipstream was investigated in [16].

The tail-sitter aircraft is a typical multi-input, multi-output, and nonlinear time-varying system with cross couplings and uncertainties. It can be regarded as a helicopter when hovering and a fixed-wing aircraft when flying forward [17]. Several control strategies have been proposed, which can be applied to achieve the desired tracking control performance. In [18], an active model based predictive control method was developed for the flight control of unmanned helicopters in full flight envelope. Similarly, a model-based tracking control design for small-scale unmanned helicopters was presented in [19]. As shown in [20], a method for using linear matrix inequalities was introduced to synthesize controller gains for a quadrotor system. In [21] and [22], the control problem of flexible spacecraft with communication delays was discussed, and distributed formation control of multiple quadrotor aircraft was proposed. In [23], a robust adaptive tracking control system for the attitude dynamics of a rigid body was presented. In [24], a feedback control strategy was proposed to make the dynamics of a class of under-actuated VTOL aircraft tracking a desired trajectory. Based on a nonlinear model of the uncertain robotic quadrotors, a robust nonlinear attitude control method was designed in [25]. However, the effects of the uncertainties to the closed-loop systems were not fully discussed in these works, and the controllers were designed based on the nonlinear systems without further analyzing of the influences of external disturbances.

The dynamics of the tail-sitter aircrafts are nonlinear with couplings, and sensitive to external disturbances. To deal with the control problem in the presence of uncertainties, various robust control techniques have been developed. In [26], a nonlinear L_2-disturbance rejection control method to a laboratory twin-rotor system was proposed for the highly nonlinear and strongly coupled dynamics. In [27], a novel asymptotic tracking controller

was introduced for an underactuated quadrotor UAV by the robust integral of the signum of the error method. To solve the multiple uncertainties control problems, the robust decentralized and linear time-invariant controller with the robust compensator was proposed to achieve trajectory tracking for quadrotors, in [28]-[29]. An adaptive compensation control scheme with disturbance observer for four-rotor helicopter was proposed in [30], to handle the attitude control problems with the unknown actuator failures and external disturbances. In [31], a new method was developed to improve the disturbance-rejection performance of a servo system by the estimation of an equivalent input disturbance. In [32], a disturbance rejection control strategy was presented for attitude tracking with disturbance observer to restrain the influences of both internal uncertainties and external disturbances. In these works, further studies on reducing the influences of uncertainties caused by parametric perturbations, external disturbances, nonlinear and coupled dynamics were not discussed fully in the stability analysis of the closed-loop control system.

In the current paper, a six-degrees-of-freedom control problem was studied for the tail-sitter aircrafts. The purpose of the control here is to improve the signal tracking capability, as well as the performance of robust stability for uncertainties including unmodeled nonlinearities, parametric uncertainties, and external disturbances. In order to design the controller for practical implementation, the system model is decoupled into a nominal model with the uncertainties parts. A robust H_∞ controller, which is low-order, linear and time-invariant, is introduced for the nominal model to achieve the desired trajectory tracking. As the effects of uncertainties on the aircraft control system cannot be reduced as desired in the whole frequency range by the standard H_∞ method, a disturbance observer is proposed for the uncertainties to improve the robustness of the closed-loop system. The proposed controller can guarantee to achieve the tracking performance and robustness against uncertainties. The simulation results show that the proposed robust control strategy can achieve better robust tracking control performance, compared with a standard H_∞ controller.

This paper is organized as follows. In Section 2, the dynamic model of the tail-sitter aircraft is presented. The robust control based on the disturbance observer method is proposed in Section 3. The stability analysis for proof of the stability of the system is shown in Section 4. The simulation comparison and conclusions are given in Section 5 and Section 6, respectively.

2. System Dynamic Model

2.1. Mechanical structure of tail-sitters

In this article, a new type tail-sitter aircraft called X-hound developed by the AOS Company is discussed. This tail-sitter aircraft consists of a fuselage, wings and a V tail as shown in Fig. 1(a). A brief outline of the aircraft is shown in Fig. 1(b). All the vanes can generate aerodynamic torques by deflection. The motors are mounted on the aircraft wings and the V tail, driving the propeller to generate thrusts, and also can generate torques by the different rates of each motor. The forces and torques generated by four rotors and four vanes can change the movements of the tail-sitter aircraft. The forces and torques for the tail-sitter aircraft during mode transition are shown in Fig. 2(a). The four rotors generate thrust and produce torques around the aerodynamic center due to the blades of rotors. The four rotors are symmetrically mounted to avoid the roll torques caused by rotors, as these moments act

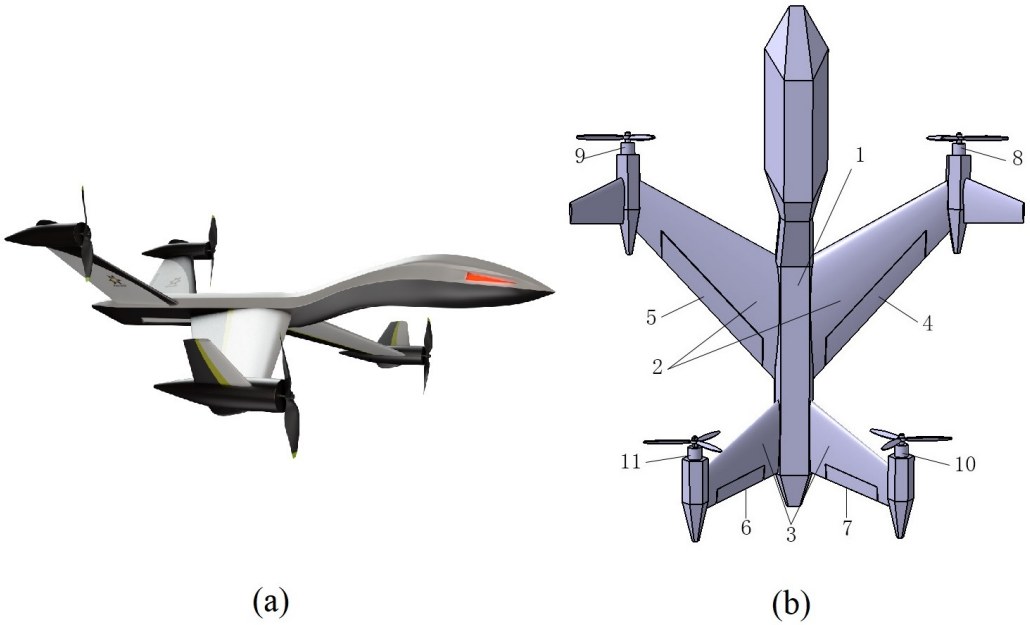

Fig. 1: X-hound vehicle: (a) X-hound tail-sitter aircraft, (b) Schematics of X-hound tail-sitter aircraft. Notations: 1: fuselage, 2: wings, 3: V tail, 4: vane 1, 5: vane 2, 6: vane 3, 7: vane 4, 8: rotor 1, 9: rotor 2, 10: rotor 3, 11: rotor 4.

in opposite direction relative to the rotation rate of the rotor. The lift forces are generated based on the layout of the aircraft, and the four vanes can adjust the aerodynamics forces and torques. In addition, the forces produced by the rotors can help increase the torques by the different rotate rates of each rotors [33]. According to change the rotor rates with the same quantity, the total thrust forces can be changed, which can affect the altitude and longitude motion of the aircraft. Depending on the desired direction, the latitude motion can be obtained by the deflection of four vanes [34]. The attitude can be maintained or changed by adjusting the rates of four rotors and the deflection of four vanes. Then the movements of the tail-sitter aircraft can be obtained.

The constraints of the tail-sitter aircraft can be mainly reflected in three parts: the flight state should be inside the range to make the aerodynamic coefficient reliable; the constraints of the actuators because of the physical limits affect the control input; the final trajectories are formulated as a terminal constraint. Then, the motion of the aircraft can be seen as the process of solving the nonlinear system under the above constraints.

2.2. Coordinates and frames

As shown in Fig. 2(b), let C be the center of gravity of the aircraft. According to the right handed inertial frame, a body fixed frame $B = \left\{ \begin{array}{ccc} B_x & B_y & B_z \end{array} \right\}$ can be obtained. And define $E = \left\{ \begin{array}{ccc} E_x & E_y & E_z \end{array} \right\}$ be an earth fixed inertial frame. The rotation matrix S_{be} from the earth fixed inertial frame E to the body fixed frame B is described as follows:

$$S_{be} = \begin{bmatrix} \cos\theta\cos\psi & \cos\theta\sin\psi & -\sin\theta \\ \sin\theta\cos\psi\sin\varphi - \sin\psi\cos\varphi & \sin\theta\sin\psi\sin\varphi - \cos\psi\cos\varphi & \cos\theta\sin\varphi \\ \sin\theta\cos\psi\cos\varphi + \sin\psi\sin\varphi & \sin\theta\sin\psi\cos\varphi - \cos\psi\sin\varphi & \cos\theta\cos\varphi \end{bmatrix},$$

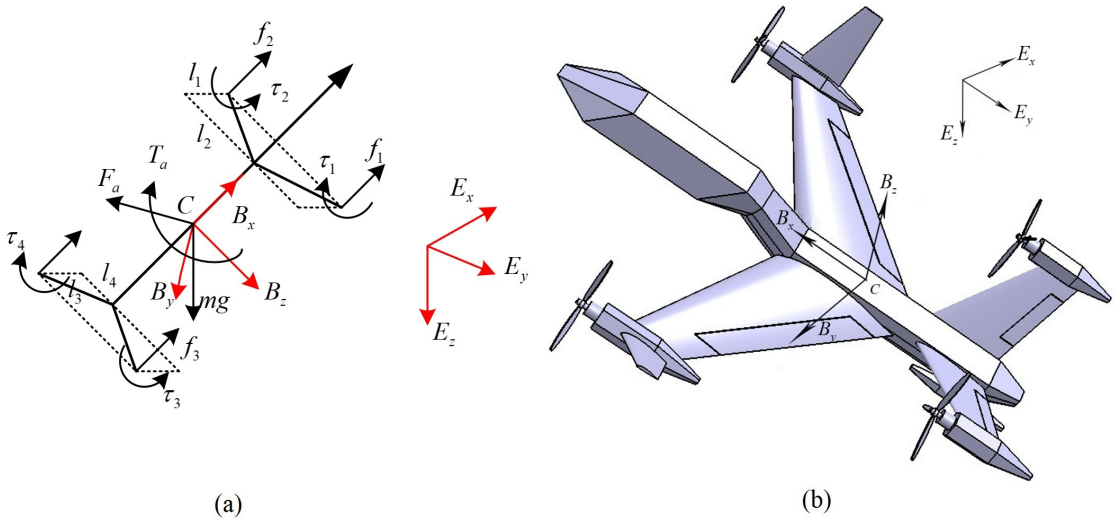

Fig. 2: X-hound Tail-sitter model: (a) Forces and torques of the aircraft during mode transition, (b) Coordinates and frames.

where Euler angles φ, θ, ψ represent roll, pitch, and yaw angle, respectively. By considering the aircraft as a rigid body model, one can obtain the dynamics equations with the following description based on Newton-Euler's law in the body frame B as

$$\begin{aligned} m\dot{v}_b &= F - S_{be}mg, \\ J\dot{\omega}_b + \omega_b^{\times} J\omega_b &= T, \end{aligned} \tag{1}$$

where m indicates the mass of the aircraft, $g = \begin{bmatrix} 0 & 0 & g_0 \end{bmatrix}$ denotes the gravitational constant, $v_b = \begin{bmatrix} v_x & v_y & v_z \end{bmatrix}^{\mathrm{T}}$, $\omega_b = \begin{bmatrix} \omega_x & \omega_y & \omega_z \end{bmatrix}^{\mathrm{T}}$ respectively represent the velocity and the angular velocity in the body frame B, $F = \begin{bmatrix} F_x & F_y & F_z \end{bmatrix}^{\mathrm{T}}$ and $T = \begin{bmatrix} T_x & T_y & T_z \end{bmatrix}^{\mathrm{T}}$ are the total force and torque. The skew-symmetric matrix $\omega_b^{\times}$ and the inertial matrix J are given as follows:

$$\omega_b^{\times} = \begin{bmatrix} 0 & -\omega_z & \omega_y \\ \omega_z & 0 & -\omega_x \\ -\omega_y & \omega_x & 0 \end{bmatrix}, J = \begin{bmatrix} J_x & -J_{xy} & -J_{xz} \\ -J_{xy} & J_y & -J_{yz} \\ -J_{xz} & -J_{yz} & J_z \end{bmatrix}.$$

The relationship between the angular velocity ω_b and the Euler angle is given by the following equation:

$$\begin{bmatrix} \omega_x \\ \omega_y \\ \omega_z \end{bmatrix} = \begin{bmatrix} -\dot{\psi}\sin\theta\cos\varphi + \dot{\varphi}\cos\theta \\ \dot{\psi}\sin\varphi + \dot{\theta} \\ \dot{\psi}\cos\varphi\cos\theta + \dot{\varphi}\sin\theta \end{bmatrix}.$$

The tail-sitter aircraft has a large maneuver in the transition mode [34]. To accurately describe the movement of the transition mode, the dynamics equations (1) can be rewritten as a more detailed expression.

Unit quaternion is adopted to describe the attitude of the aircraft in order to avoid the drawback of using Euler angle which may result in the singularity problem. The quaternions have been used in the actual model part. However, to facilitate the design of the controller and reading, the quaternions have been transformed into Euler angles, and simulation results are also described by Euler angles to analysis the robust stability and robust tracking properties of the closed-loop systems.

2.3. Dynamical model

The dynamics equations of the aircraft are established in the body fixed frame B. From (1), the nonlinear kinetic equations and kinematics equations are obtained as follows:

$$\begin{aligned}
\dot{v}_x &= v_y\omega_z - v_z\omega_y - g\sin\theta + F_x/m,\\
\dot{v}_y &= -v_x\omega_z + v_z\omega_x + g\cos\theta\sin\varphi + F_y/m,\\
\dot{v}_z &= v_x\omega_x - v_y\omega_y + g\cos\theta\cos\varphi + F_z/m,\\
\dot{\omega}_x &= (c_1\omega_z + c_2\omega_x)\omega_y + c_3T_x + c_4T_z,\\
\dot{\omega}_y &= c_5\omega_x\omega_z - c_6({\omega_x}^2 - {\omega_z}^2) + c_7T_y,\\
\dot{\omega}_z &= (c_8\omega_x - c_2\omega_z)\omega_y + c_4T_x + c_9T_z,
\end{aligned} \tag{2}$$

where the coefficients $c_i (i = 1 \sim 9)$ are constant parameters. The total force F is composed of three parts: the thrust F_m generated by the four motors, the aerodynamic force $F_a = \begin{bmatrix} F_{ax} & F_{ay} & F_{az} \end{bmatrix}^{\mathrm{T}}$, and the external disturbances $d_v = \begin{bmatrix} d_{vx} & d_{vy} & d_{vz} \end{bmatrix}^{\mathrm{T}}$. By considering the four rotors mounted parallel to the body fixed frame axis B_x, the thrust F_m can be expressed as $F_m = \begin{bmatrix} F_{mx} & 0 & 0 \end{bmatrix}^{\mathrm{T}}$. Hence these forces are described in body fixed frame B as follow:

$$\begin{bmatrix} F_x \\ F_y \\ F_z \end{bmatrix} = \begin{bmatrix} F_{mx} + F_{ax} + d_{vx} \\ F_{ay} + d_{vy} \\ F_{az} + d_{vz} \end{bmatrix}.$$

Similarly to the expression of the total force, the total torque T consists of the torque $T_m = \begin{bmatrix} T_{mx} & T_{my} & T_{mz} \end{bmatrix}^{\mathrm{T}}$ from the four rotors, the aerodynamic torque $T_a = \begin{bmatrix} T_{ax} & T_{ay} & T_{az} \end{bmatrix}^{\mathrm{T}}$ from the deflection of the four vanes, and the external disturbances $d_\omega = \begin{bmatrix} d_{\omega x} & d_{\omega y} & d_{\omega z} \end{bmatrix}^{\mathrm{T}}$. Let $k = |v_b - v_0|/|v_e - v_0|$ be the parameter that adjusts the proportions of T_m and T_a to avoid the low aerodynamic efficiency in hover or low speed state, where v_0 indicates the speed of hover state, and v_e is the speed of fly forward state. Then the following expression can be obtained:

$$\begin{bmatrix} T_x \\ T_y \\ T_z \end{bmatrix} = \begin{bmatrix} (1-k)T_{mx} + kT_{ax} + d_{\omega x} \\ (1-k)T_{my} + kT_{ay} + d_{\omega y} \\ (1-k)T_{mz} + kT_{az} + d_{\omega z} \end{bmatrix}.$$

Due to the low aerodynamic efficiency in hover or low speed state of the tail-sitter aircraft, both the rotors and the vanes should be used to achieve the desired mode transition. Since there are more control effectors than the control inputs, an allocation algorithm should be used to obtain a unique solution of the control inputs. Several related papers have proposed complicated algorithms to distribute the control input, as shown in [35]-[36]. In fact, the

control distribution problem between aerodynamic and motor torques requires more complicated nonlinear algorithms for better performance. But, the linear algorithm is able to achieve a reasonable allocation between these two moments and thereby a simplified linear form is applied. In this paper, in order to simplify the distribution algorithms and make it easy to be implemented in practical applications, the parameter k is introduced to adjust the proportions of total torque and the expression $k = |v_b - v_0|/|v_e - v_0|$ is given as a linear form to denote the approximately relationship between the two torques. The parameter k should be in the range of $0 \leq k \leq 1$ and only valid during transition phase. The thrust F_m and the torque T_m caused by the rotors can be described as:

$$
\begin{aligned}
F_{mx} &= \lambda_1(\varpi_1^2 + \varpi_2^2 + \varpi_3^2 + \varpi_4^2),\\
T_{mx} &= \lambda_2(\varpi_1^2 - \varpi_2^2 - \varpi_3^2 + \varpi_4^2),\\
T_{my} &= \lambda_2(\varpi_1^2 l_1 + \varpi_2^2 l_1 - \varpi_3^2 l_2 - \varpi_4^2 l_2),\\
T_{mz} &= \lambda_2(\varpi_1^2 l_3 - \varpi_2^2 l_3 + \varpi_3^2 l_4 - \varpi_4^2 l_4).
\end{aligned}
$$

where $\lambda_i (i = 1, 2)$ are constant coefficients, $l_i (i = 1, 2, 3, 4)$ represent the distance between the mass center and the rotors, $\varpi_i (i = 1, 2, 3, 4)$ denote the rotation rates of each rotors, respectively. The aerodynamic force F_a and torque T_a are expressed as follows:

$$
\begin{cases} F_{ax} = \rho |v_b|^2 S C_X/2 \\ F_{ay} = \rho |v_b|^2 S C_Y/2 \\ F_{az} = \rho |v_b|^2 S C_Z/2 \end{cases}, \begin{cases} T_{ax} = \rho |v_b|^2 c S C_R/2 \\ T_{ay} = \rho |v_b|^2 c S C_M/2 \\ T_{az} = \rho |v_b|^2 c S C_N/2 \end{cases},
$$

where ρ denotes the reference atmospheric density, $|v_b| = (v_x^2 + v_y^2 + v_z^2)^{1/2}$ indicates the reference speed of the aircraft, c represents the reference wing chord length, S is the reference aircraft pneumatic area, and $C_i (i = X, Y, Z, R, M, N)$ specify the aerodynamic coefficients. The aerodynamic coefficients are obtained by the interpolation from the aerodynamic database at different working conditions. The database has been established by computational fluid dynamics calculation. The approximate aerodynamic coefficient parametric formulas can be expressed as follows:

$$
\begin{aligned}
C_X &= C_{X_0} + C_{X_1}\alpha,\\
C_Y &= C_{Y_0} + C_{Y_1}\beta,\\
C_Z &= C_{Z_0} + C_{Z_1}\alpha,\\
C_R &= C_{R_0} + C_{R_1}\beta + C_{R_2}(\delta_1 + \delta_2),\\
C_M &= C_{M_0} + C_{M_1}\alpha + C_{M_2}(\delta_3 + \delta_4),\\
C_N &= C_{N_0} + C_{N_1}\beta + C_{N_2}(\delta_3 - \delta_4),
\end{aligned}
$$

where $\alpha = \arctan(v_z/v_x)$ denotes the angle of attack, $\beta = \arcsin(v_y/|v_b|)$ is the sideslip angle, and $\delta_i (i = 1, 2, 3, 4)$ represent the deflection of the four vanes, respectively.

To ensure the effectiveness of the aerodynamics, the state constraints in the model transition can be described as $\alpha_{\min} < \alpha < \alpha_{\max}$ and $|\beta| < \beta_{\lim}$, where $\alpha_{\min} = -5^\circ$, $\alpha_{\max} = 15^\circ$, and $\beta_{\lim} = 10^\circ$. If the flight state is outside the range, the aerodynamic coefficients would be unreliable. In the situation of the failures of the aerodynamics effectiveness, the flight control of the aircraft is mainly achieved by the rotors.

Furthermore, the attitude control is implemented based on the moments generated by both the propellers and vanes. Because the size of the propeller is restricted, the deflection

of the vanes is within a certain range. The flying velocity of the aircraft is required to attain a given value which can provide the sufficient moments in the level and vertical flying modes. Therefore, the control laws need to satisfy the physical constraints of the tail-sitter aircraft and incorporate the actuator limits of the aircraft. The saturation constraints and loads make the rotors exist physical limits as $0 < \varpi_i < \varpi_{\max},\ \ i = 1, 2, 3, 4.$ and the vanes also have the constraint of the maximum deflection angle as $|\delta_i| < \delta_{\max},\ \ i = 1, 2, 3, 4,$ where $\varpi_{\max} = 12000r/\min$ and $\delta_{\max} = 20°$. Thus a reasonable control method should be established for avoiding the limits of the actuators.

Remark 1. From above equations, the movements of the tail-sitter aircraft can be obtained. Once the rotation rates of the four rotors and the deflection of the vanes are determined, the forces and torques can be given. However, this dynamics model still exists nonlinearities and coupling terms. The nominal model should be established for the controller design.

According to the actual situation and the characteristics of the aircraft, a nominal model in fly forward state can be built. Define the control inputs as:

$$
\begin{aligned}
u_v &= \lambda_1(\varpi_1^2 + \varpi_2^2 + \varpi_3^2 + \varpi_4^2),\\
u_\varphi &= \lambda_2(1-k)(\varpi_1^2 - \varpi_2^2 - \varpi_3^2 + \varpi_4^2) + (k\rho|v_b|^2 cS\,C_{R_2}(\delta_1 + \delta_2))/2,\\
u_\theta &= \lambda_2(1-k)(\varpi_1^2 l_1 + \varpi_2^2 l_1 - \varpi_3^2 l_2 - \varpi_4^2 l_2) + (k\rho|v_b|^2 cS\,C_{M_2}(\delta_3 + \delta_4))/2,\\
\delta_\psi &= \lambda_2(1-k)(\varpi_1^2 l_3 - \varpi_2^2 l_3 + \varpi_3^2 l_4 - \varpi_4^2 l_4) + (k\rho|v_b|^2 cS\,C_{N_2}(\delta_3 - \delta_4))/2.
\end{aligned}
$$

The parameter k should be satisfied: when the flight speed is large enough, the aircraft should be mainly controlled by the aerodynamic torque to save the energy; when in the low flight speed state, the attitude control is mainly performed by the rotors to avoid the inefficiency of the aerodynamic torque; when the aerodynamic torque is large, but not enough to fully control the aircraft, the parameter k would correctly distribute the control torque to the rotors and the vanes that they can generate corresponding torques to achieve the desired attitude control within their physical limits. It can be seen that the four control inputs $u_i(i = v, \varphi, \theta, \psi)$ are linearly related to F_x, T_x, T_y, and T_z. Then the nonlinear system model (2) can be rewritten as:

$$
\begin{aligned}
\dot{v}_x &= b_x u_v + q_x,\\
\dot{v}_y &= b_y \beta + q_y,\\
\dot{v}_z &= b_z \alpha + q_z,\\
\dot{\omega}_x &= b_x^\varphi u_\varphi + b_x^\psi u_\psi + q_\varphi,\\
\dot{\omega}_y &= b_y^\theta u_\theta + q_\theta,\\
\dot{\omega}_z &= b_z^\varphi u_\varphi + b_z^\psi u_\psi + q_\psi,
\end{aligned}
\tag{3}
$$

where $b_x = 1/m$, $b_y = \rho v_e S C_{Y_1}/2m$, $b_z = \rho v_e S C_{Z_1}/2m$, $b_x^\varphi = c_3$, $b_x^\psi = c_4$, $b_y^\theta = c_7$, $b_z^\varphi = c_4$, $b_z^\psi = c_9$. Denote the equivalent disturbances $q_i(i = x, y, z, \varphi, \theta, \psi)$ and the following expression can be obtained:

$$
\begin{aligned}
q_x &= v_y\omega_z - v_z\omega_y - g\sin\theta + \tfrac{1}{m}F_{ax} + \tfrac{1}{m}d_{vx},\\
q_y &= -v_x\omega_z + v_z\omega_x + g\cos\theta\sin\varphi + \tfrac{1}{2m}\rho v_b^2 S\,C_{Y_0} + \tfrac{1}{m}d_{vy},\\
q_z &= v_x\omega_x - v_y\omega_y + g\cos\theta\cos\varphi + \tfrac{1}{2m}\rho v_b^2 S\,C_{Z_0} + \tfrac{1}{m}d_{vz},\\
q_\varphi &= (c_1\omega_z + c_2\omega_x)\omega_y + \tfrac{c_3 k}{2}\rho v_b^2 cS\,(C_{R_0} + C_{R_1}\beta) + \tfrac{c_4 k}{2}\rho v_b^2 cS\,(C_{N_0} + C_{N_1}\beta) + d_\varphi,\\
q_\theta &= c_5\omega_x\omega_z - c_6({\omega_x}^2 - {\omega_z}^2) + \tfrac{c_7 k}{2}\rho v_b^2 cS\,(C_{M_0} + C_{M_1}\alpha) + d_\theta,\\
q_\psi &= (c_8\omega_x - c_2\omega_z)\omega_y + \tfrac{c_4 k}{2}\rho v_b^2 cS\,(C_{R_0} + C_{R_1}\beta) + \tfrac{c_9 k}{2}\rho v_b^2 cS\,(C_{N_0} + C_{N_1}\beta) + d_\psi.
\end{aligned}
$$

It can be seen that there exist coupling and nonlinearities in the model. The couplings and nonlinearities existed in the model address a challenging controller design problem for the tail-sitter aircrafts. The disturbances $d_i(i = x, y, z, \varphi, \theta, \psi)$ can be seen as the additional forces torques mainly caused by the external wind gusts. One can see that the tail-sitter aircraft is a typical multi-input, multi-output, and nonlinear time-varying system with cross couplings and uncertainties.

It has been shown that the angle of attack is within a reasonable range when the vehicle reaches a high flight speed. Furthermore, the angle of attack will change drastically during the situation such as hover state, because the velocity v_x is almost 0. However, the tail-sitter aircraft is mainly controlled by the propellers in the low speed state, which could avoid the aerodynamic problem caused by the excessive angle of attack. As for the transition mode, both the rotors and the vanes are used to achieve the desired trajectories. The rotors are the main actuators to generate the control torque by the proportion of allocation parameter k and the simulation results show that the stall constraint does not occur during the transition mode. If the flight state is outside the range, the aerodynamic coefficients would be unreliable. In the situation of the failures of the aerodynamics effectiveness, the flight control of the aircraft is mainly achieved by the rotors. Therefore, the stall problem caused by angle of attack is not further discussed.

Remark 2. It can be seen that the equivalent disturbances $q_i(i = x, y, z, \varphi, \theta, \psi)$ contain nonlinearities, uncertainties, and disturbances. It should be noted that the equivalent disturbances are different from the input disturbances.

Remark 3. From the nonlinear model (2), it can be seen that the system contains the linear terms involving the control inputs and other terms. The nominal model can be obtained from the nonlinear system model by selecting the dominant linear, time-invariant terms, while the others including coupling terms, uncertainties, and external disturbances are included in the equivalent disturbances. For example, the first equation of mode (2) is $\dot{v}_x = v_y\omega_z - v_z\omega_y - g\sin\theta + F_x/m$. This term can be divided into the nominal linear part $\lambda_1(\varpi_1^2+\varpi_2^2+\varpi_3^2+\varpi_4^2)/m$, which can be controlled by the input $u_v = \lambda_1(\varpi_1^2+\varpi_2^2+\varpi_3^2+\varpi_4^2)$, and the equivalent disturbance part $v_y\omega_z - v_z\omega_y - g\sin\theta + F_{ax}/m + d_x/m$.

3. Controller Design

As the nonlinear model (3) has been obtained from the last section, the nominal model can be given by ignoring the equivalent disturbances $q_i(i = x, y, z, \varphi, \theta, \psi)$. Then as shown in Fig. 3, a controller composed of robust H_∞ controller and nonlinear disturbance observer is proposed in this section. The robust H_∞ controller including a position loop and an attitude loop is designed based on the nominal model to achieve the desired trajectory tracking. The nonlinear disturbance observer involved the nonlinear dynamics equations is introduced for restraining the influence of the equivalent disturbances.

The control inputs $u_i(i = v, \varphi, \theta, \psi)$ are consisted of two parts as follows:

$$u_i = u_i^{H_\infty} + u_i^D, \quad i = v, \varphi, \theta, \psi \tag{4}$$

where $u_i^{H_\infty}(i = v, \varphi, \theta, \psi)$ denote the H_∞ control inputs, and $u_i^D(i = v, \varphi, \theta, \psi)$ represent the nonlinear disturbance observer control inputs.

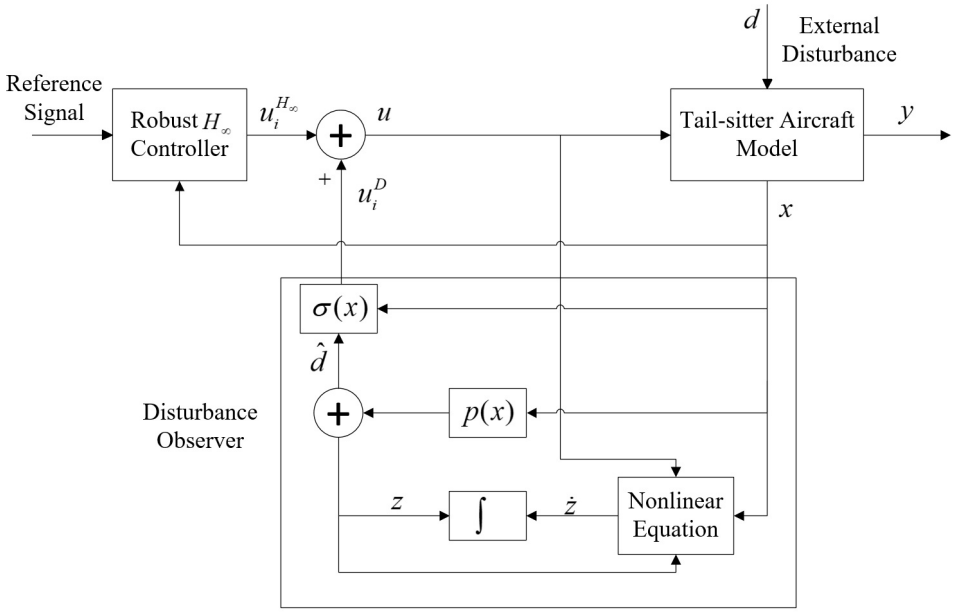

Fig. 3: Control structure of the proposed controller.

Take the pitch angle as an example, the reference signals can be obtained by following equations:

$$\omega_{f\theta} = \begin{cases} \sqrt{2a_{\max}(|\theta_r - \theta_R[k]| - \frac{\theta_l}{2})}, & \theta_r - \theta_R[k] > \theta_l, \\ K_{gain}(\theta_r - \theta_R[k]), & |\theta_r - \theta_R[k]| \le \theta_l, \\ -\sqrt{2a_{\max}(|\theta_r - \theta_R[k]| - \frac{\theta_l}{2})}, & \theta_r - \theta_R[k] < -\theta_l, \end{cases}$$

where $\omega_{f\theta}$ represents the feed forward angular velocity of pitch angle, $a_{\max}$ is the maximum angular acceleration determined by the physical characteristics of the aircraft, θ_r denotes the desired reference pitch angle, $\theta_R[k]$ indicates the trajectory pitch angle for the k-th iteration, K_{gain} is a positive constant value, and $\theta_l = a_{\max}/K_{gain}$. It can be seen that the linear approximation is applied when the error between the desired reference signal and trajectory pitch angle less than θ_l. Otherwise, a constant acceleration approach is used to protect the rotors and vanes. Define Δt be the interval between iterations, the trajectory pitch angle can be given by iterative calculation:

$$\theta_R[k+1] = \theta_R[k] + \omega_{f\theta}\Delta t.$$

3.1. H_∞ controller design

Denote tracking errors as follow:

$$\begin{aligned} e_v &= v_x - v_R \\ e_\varphi &= \varphi - \varphi_R, \\ e_\theta &= \theta - \theta_R, \\ e_\psi &= \psi - \psi_R, \end{aligned}$$

and define $E_i\,(i = v, \varphi, \theta, \psi)$ as:

$$E_v = \begin{bmatrix} e_V \\ e_v \end{bmatrix}, \dot{e}_V = e_v,$$
$$E_j = \begin{bmatrix} e_j \\ \dot{e}_j \end{bmatrix}, j = \varphi, \theta, \psi,$$

where v_R, φ_R, θ_R, and ψ_R are the reference tracking signals. Let $Z_i\,(i = v, \varphi, \theta, \psi)$ be the controlled outputs to evaluate the controller performance by the weighting matrices C_i and D_i. Similar to [37], the following expressions can be obtained according to the nominal error tracking model with the equivalent disturbances:

$$\begin{aligned} &\dot{E}_i = A_i E_i + B_i u_i^{H\infty} + M_i q_i, \\ &Z_i = C_i E_i + D_i u_i^{H\infty}, \quad i = v, \varphi, \theta, \psi \end{aligned} \tag{5}$$

where

$$A_i = \begin{bmatrix} 0 & 1 \\ 0 & 0 \end{bmatrix}, B_i = \begin{bmatrix} 0 \\ b_i \end{bmatrix}, M_i = \begin{bmatrix} 0 \\ 1 \end{bmatrix},$$

$$C_i = \begin{bmatrix} r_1^i & 0 \\ 0 & r_2^i \\ 0 & 0 \end{bmatrix}, D_i = \begin{bmatrix} 0 \\ 0 \\ r_3^i \end{bmatrix},$$

and r_1^i, r_2^i, r_3^i are weighting parameters. The specified values will be given later. Then, the H_∞ controller inputs can be given by:

$$u_i^{H\infty} = K_i E_i, \quad i = v, \varphi, \theta, \psi \tag{6}$$

where $K_i (i = v, \varphi, \theta, \psi)$ are the gains of the H_∞ state feedback control and have the following forms:

$$K_i = \begin{bmatrix} k_1^i & k_2^i \end{bmatrix}, \quad i = v, \varphi, \theta, \psi$$

Let s be the Laplace operator, then one can obtain the closed-loop transfer function of each channel as follows:

$$T_{zw,i}(s) = (C_i + D_i K_i)\,(sI - A_i - B_i K_i)^{-1} M_i, \quad i = v, \varphi, \theta, \psi. \tag{7}$$

If the pairs are stabilizable, for the given $\gamma_i > \gamma_i^*$, there exist static state-feedback gains K_i such that $A_{\mathrm{cld}} = A_i + B_i K_i$ are asymptotically stable, and $\left\| T_{zw,i}(s) \right\|_\infty \leq \gamma_i$ if and only if there exist matrices $Q_i = Q_i^T > 0$ and $P_i = P_i^T > 0$ such that:

$$\begin{aligned} &A_{ei}^T P_i + P_i A_{ei} + P_i \left(\gamma^{-2} D_{ei} D_{ei}^T - B_{ei} B_{ei}^T \right) P_i + C_{ei} C_{ei}^T + Q_i = 0, \\ &K_i = -B_{ei}^T P_i, \quad i = 1, 2, 3 \end{aligned}$$

where $\gamma_i^* = \min_{K_i} \left\| T_{zw,i}(s) \right\|_\infty$. Then, one can get the necessary and sufficient conditions for the existence of the H_∞ suboptimal state-feedback gains, and obtain the gain matrices K_i of the H_∞ controller. $B_{ei} (i = 1, 2, 3)$ are nonzero in the actual aircraft parameters. As the pairs $(A_{ei},\ B_{ei})$ are controllable, one can obtain that $A_i (i = 1, 2, 3)$ are Hurwitz.

3.2. Nonlinear disturbance observer design

As shown in [38]-[39], the disturbance observer is designed to suppress the uncertainties. The nonlinear system model of the aircraft dynamics has been given from (3). To facilitate the design of the nonlinear disturbance observe, the nonlinear model can be rewritten as following expression:

$$\begin{aligned} &\dot{x} = f(x) + g(x)u + m(x)d, \\ &y = h(x), \end{aligned} \tag{8}$$

where $x = \begin{bmatrix} v_x & \omega_x & \omega_y & \omega_z \end{bmatrix}^{\mathrm{T}}$ denotes the state vector, $u = \begin{bmatrix} u_v & u_\varphi & u_\theta & u_\psi \end{bmatrix}^{\mathrm{T}}$ is the control input, $d = \begin{bmatrix} d_{vx} & d_{\omega x} & d_{\omega y} & d_{\omega z} \end{bmatrix}^{\mathrm{T}}$ represents the external disturbance, $y = \begin{bmatrix} v_x & \varphi & \theta & \psi \end{bmatrix}^{\mathrm{T}}$ indicates the output term. To the terms of state vector x, assuming $f(x)$, $g(x)$, $m(x)$, $h(x)$ are smooth functions, and

$$f(x) = \begin{bmatrix} v_y\omega_z - v_z\omega_y - g\sin\theta + \frac{1}{m}F_{ax} \\ (c_1\omega_z + c_2\omega_x)\omega_y + \frac{c_3k}{2}\rho v_b^2 cS(C_{R_0} + C_{R_1}\beta) + \frac{c_4k}{2}\rho v_b^2 cS(C_{N_0} + C_{N_1}\beta) \\ c_5\omega_x\omega_z - c_6({\omega_x}^2 - {\omega_z}^2) + \frac{c_7k}{2}\rho v_b^2 cS(C_{M_0} + C_{M_1}\alpha) \\ (c_8\omega_x - c_2\omega_z)\omega_y + \frac{c_4k}{2}\rho v_b^2 cS(C_{R_0} + C_{R_1}\beta) + \frac{c_9k}{2}\rho v_b^2 cS(C_{N_0} + C_{N_1}\beta) \end{bmatrix},$$

$$g(x) = \begin{bmatrix} b_x & 0 & 0 & 0 \\ 0 & b_x^\varphi & 0 & b_x^\psi \\ 0 & 0 & b_y^\theta & 0 \\ 0 & b_z^\varphi & 0 & b_z^\psi \end{bmatrix}, m(x) = \begin{bmatrix} \frac{1}{m} & 0 & 0 & 0 \\ 0 & 1 & 0 & 0 \\ 0 & 0 & 1 & 0 \\ 0 & 0 & 0 & 1 \end{bmatrix},$$

$$h(x) = \begin{bmatrix} v_x \\ \int(\omega_x\cos\theta + \omega_z\sin\theta)dt \\ \int(\omega_x\sin\theta\tan\varphi + \omega_y - \omega_z\cos\theta\tan\varphi)dt \\ \int(-\omega_x\frac{\sin\theta}{\cos\varphi} + \omega_z\frac{\cos\theta}{\cos\varphi})dt \end{bmatrix}.$$

The nonlinear disturbance observer is introduced to estimate the external disturbance d. Let $\hat{d}$ be the estimated value of the external disturbances, and the expression is given as:

$$\begin{aligned} &\hat{d} = z + p(x), \\ &\dot{z} = -l(x)m(x)z - l(x)[m(x)p(x) + f(x) + g(x)u], \\ &l(x) = \frac{\partial p(x)}{\partial(x)}, \end{aligned} \tag{9}$$

where z specifies the state vector of the nonlinear disturbance observer, $p(x)$ denotes a smooth function given as:

$$\begin{aligned} &e_d = d - \hat{d}, \\ &\dot{e}_d + \frac{\partial p(x)}{\partial(x)}m(x)e_d = 0. \end{aligned} \tag{10}$$

From (9) and (10), the estimate value $\hat{d}$ of the external disturbances can be obtained. Let the nonlinear disturbance observer control inputs $u_i^D (i = v, \varphi, \theta, \psi)$ be:

$$u^D = \begin{bmatrix} u_v^D & u_\varphi^D & u_\theta^D & u_\psi^D \end{bmatrix}^{\mathrm{T}} = \sigma(x)\hat{d}, \tag{11}$$

where $\sigma(x)$ is the compensation gain of the observer. To design the compensation gain $\sigma(x)$, the nonlinear model equation (8) can be described as:

$$\begin{aligned} &\dot{x} = \bar{f}(x)x + g(x)u + m(x)d, \\ &y = \bar{h}(x)x, \\ &u^{H_\infty} = \begin{bmatrix} u_\nu^{H_\infty} & u_\varphi^{H_\infty} & u_\theta^{H_\infty} & u_\psi^{H_\infty} \end{bmatrix}^{\mathrm{T}}, \\ &u = \bar{u}^{H_\infty}(x)x + \sigma(x)\hat{d}, \end{aligned} \tag{12}$$

where $\bar{f}(x) = f(x)/x$, $\bar{h}(x) = h(x)/x$, and $\bar{u}^{H_\infty}(x) = u^{H_\infty}(x)/x$. They are diagonal matrices such as

$$\begin{aligned} f(x) &= \begin{bmatrix} f_1(x) & f_2(x) & f_3(x) & f_4(x) \end{bmatrix}^T, \\ x &= \begin{bmatrix} x_1 & x_2 & x_3 & x_4 \end{bmatrix}^T, \\ \bar{f}(x) &= \begin{bmatrix} f_1(x)/x_1 & 0 & 0 & 0 \\ 0 & f_2(x)/x_2 & 0 & 0 \\ 0 & 0 & f_3(x)/x_3 & 0 \\ 0 & 0 & 0 & f_4(x)/x_4 \end{bmatrix}. \end{aligned}$$

The state vector x can be rewritten as:

$$x = \left[\bar{f}(x) + g(x)\bar{u}^{H_\infty}\right]^{-1} \left\{\dot{x} - g(x)\sigma(x)e_d - \left[g(x)\sigma(x) + m(x)\right]d\right\},$$

and combining $y = \bar{h}(x)x$, the compensation gain $\sigma(x)$ can be given as:

$$\sigma(x) = -\left\{\bar{h}(x)\left[\bar{f}(x) + g(x)\bar{u}^{H_\infty}\right]^{-1} g(x)\right\} \times \bar{h}(x)\left[\bar{f}(x) + g(x)\bar{u}^{H_\infty}(x)\right]^{-1} m(x), \tag{13}$$

then substituting the compensation gain $\sigma(x)$ to the model (12), the following expression can be obtained:

$$y = \bar{h}(x)\left[\bar{f}(x) + g(x)\bar{u}^{H_\infty}\right]^{-1}\dot{x} + \bar{h}(x)\left[\bar{f}(x) + g(x)\bar{u}^{H_\infty}\right]^{-1} m(x)e_d.$$

If the external disturbance d and its derivative $\dot{d}$ are bounded and the closed loop system is stable, it can be seen that the influences of the external disturbances are restrained. The stability analysis of the closed loop system are introduced in Section 4.

Remark 4. It should be noted that the nonlinear disturbance observer based on equivalent input disturbances is mainly utilized to restrain the influence of disturbances. If the system is a nominal model that the uncertainties are ignored, it can be seen that the disturbance observer would not generate any control inputs.

4. Stability Analysis

Denote the equivalent disturbance d be the inputs of the nonlinear system, x represent the system state, and e specify the observer state. The input-to-state stability of the nonlinear system can be proven by the following lemma and theorem.

Let $\bar{x} = \begin{bmatrix} x & e_d \end{bmatrix}^T$, $F(\bar{x}) = \begin{bmatrix} f(x) + g(x)u - g(x)\beta(x)e_d & -l(x)m(x)e_d \end{bmatrix}^T$, and define a continuous function R, which is strictly increasing in interval $[0, a)$, where a is a positive constant value and satisfied $R(0) = 0$. The function R can be called to belong to class κ. And in condition that $\lim_{a\to\infty} R(a) = \infty$, the continuous function R can be seen to belong to class κ_∞.

Lemma 1. *Considering a nonlinear system as $\dot{x} = F(x, u)$, where x, u represent the state vector and control input, respectively. Assuming the equilibrium condition $x = 0$ of $\dot{x} = f(x, 0)$ is global asymptotically stable. Then there exists a n dimensional matrix $N(x)$ of smooth functions of x to make the nonlinear system be input to state stable (ISS), which is nonsingular and defined for all x, such that:*

$$\dot{x} = F(x, N(x)u). \tag{14}$$

Proof. According to the converse Lyapunov theorem, there exists a positive definite and proper function $V(x)$ and a class κ_∞ function R such that:

$$\frac{\partial V}{\partial x} F(x, 0) < -R(\|x\|),$$

where $\|\cdot\|$ denotes the Euclidean norm of a vector. The theorem can be proven by showing that: for any $N(x)$ having the properties indicated above and for some class κ function χ, if $\|x\| \geq \chi(\|u\|)$, then there exists:

$$\frac{\partial V}{\partial x} F(x, N(x)u) \leq -\frac{1}{2} R(\|x\|). \tag{15}$$

Thus showing that $V(x)$ is an ISS-Lyapunov function for system (14). Let $G(\cdot)$ be any smooth function which is positive and identically equal to 1 on the interval $[0, 1]$, and let $N(x) = G(\|x\|)I$, where I is the unit matrix. The matrix $N(x)$ thus defined is a matrix of smooth functions of x and invertible. Define

$$\delta(s, \tau) = \max_{\|x\|=s,\ \|\mu\|=\tau} \{\frac{\partial V}{\partial x} f(x, \mu) + \frac{1}{2}\mathrm{R(s)}\},$$

and

$$\frac{\partial V}{\partial x} F(x, N(x)u) + \frac{1}{2} R(\|x\| \leq \delta(\|x\|, G(\|x\|)\|u\|), \tag{16}$$

for all x and u. The function $\delta(s, \tau)$, a continuous function defined for all (s, τ), by hypothesis is such that $\delta(s, 0) < 0$ for every $s > 0$. Thus, by using continuity arguments, it can be proven that there exist a continuous function $\rho(s)$, defined for all $s \geq 0$, with $\rho(0) = 0$ and $\rho(s) > 0$ for all $s > 0$, such that $\tau \leq \rho(s) \Rightarrow \delta(s, \tau) < 0$ for all $s > 0$. In view of this and of (16), the result is proven if one can show the existence of a function $\chi(\cdot)$ and complete the definition of $G(\cdot)$ so that:

$$\|x\| \geq \chi(\|u\|) \Rightarrow G(\|x\|)\|u\| \leq \rho(\|x\|). \tag{17}$$

Let $\vartheta(\cdot)$ be any class κ_∞ function which satisfies: $\vartheta(s) < \rho(s)$ for $s \leq 2$, $\vartheta(s) < s$ for $s > 2$, and $\chi(s) = \vartheta^{-1}(s)$. Moreover, let $G(\cdot)$ be $G(s) \leq 1$ for all s. By construction, the functions $\vartheta(\cdot)$ and $G(\cdot)$ are such that: $G(s)\vartheta(s) \leq \rho(s)$ for all s. Observe now that:

$$\|x\| \geq \chi(\|u\|) \Rightarrow \vartheta(\|x\|) \geq \|u\|.$$

Therefore,

$$\|x\| \geq \chi(\|u\|) \Rightarrow G(\|x\|)\|u\| \leq G(\|x\|)\vartheta(\|x\|) \leq \rho(\|x\|), \tag{18}$$

which shows that (17) holds and this completes the proof. □

It can be observed easily that the linearized nominal model is controllable, while the stability of the closed-loop system should be proven clearly. The external disturbances are supposed to be harmonic ones with known frequency mainly, but unknown amplitude and phase rather than constant ones. It is assumed that the disturbances are generated by the following system:

$$\begin{aligned}\dot{\xi} &= A\xi,\\ d &= C\xi.\end{aligned}$$

where $\xi_i \in R$.

Theorem 1. *Considering the system (3) under the external disturbances $d_i(i = x, y, z, \varphi, \theta, \psi)$, the nonlinear disturbance observer (9) can exponentially estimate the disturbances and be globally exponentially stable regardless of x.*

Proof. Let the nonlinear observer gain $l(x)$ be selected as $\dot{e}_d + [A - l(x)m(x)e_dC] = 0$. Then the observation error dynamics can be given:

$$\begin{aligned}\dot{e}_d &= \dot{d} - \dot{\hat{d}}\\ &= Ad - \dot{z} - l(x)\dot{x}\\ &= Ad - [A - l(x)m(x)C]z - Ap(x) + l(x)[m(x)Cp(x)\\ &\quad + f(x) + g(x)u] - l(x)[f(x) + g(x)u + m(x)d]\\ &= [A - l(x)m(x)C](d - \hat{d})\\ &= [A - l(x)m(x)C]e_d.\end{aligned} \tag{19}$$

It can be seen from (19) that the $\hat{d}$ can approaches d exponentially under the selected $l(x)$. Supposed the relative degree r from the disturbance to the output is uniformly well-defined. Therefore, it can be obtained that $L_mL_f^{r-1}h(x) \neq 0$ for all x, where L denotes Lie derivatives. Let $L_mL_f^{r-1}h(x) > 0$ and then $L_mL_f^{r-1}h(x)$ can be divided as

$$L_mL_f^{r-1}h(x) = \alpha_0 + \alpha_1(x), \tag{20}$$

where $\alpha_0 > 0$ is a constant that can be chosen as the minimum of $L_mL_f^{r-1}h(x)$ over all x, and $\alpha_1(x) > 0$ for all x as well. The nonlinear function $p(x)$ of the disturbance observer can be given as

$$p(x) = KL_f^{r-1}h(x)$$

where K is the gain to be determined. From (9), it can be obtained that $l(x) = \frac{\partial p(x)}{\partial x} = K\frac{L_f^{r-1}h(x)}{\partial x}$.

According to the above equations, the observation error dynamics (19) can be rewritten as:

$$\begin{aligned}\dot{e}_d &= [A - K\frac{L_f^{r-1}h(x)}{\partial x}m(x)C]e_d\\ &= [A - KL_mL_f^{r-1}h(x)C]e_d\\ &= [A - K(\alpha_0 + \alpha_1(x))C]e_d.\end{aligned}$$

Let $\bar{A} = A - K\alpha_0 C$. One can see that there exists a positive definite matrix P which satisfied $\bar{A}^T P + P\bar{A} < 0$ and $PK = C^T$.A Lyapunov candidate function for observation error dynamics can be defined as $V(e_d) = e_d^T P e_d$. According to the derivative of the Lyapunov function with respect to time along the trajectory of observer error dynamics, the following expression can be given:

$$\begin{aligned} V(e_d) &= 2e_d^T P[A - K(\alpha_0 + \alpha_1(x))C]e_d \\ &= e_d^T(\bar{A}^T P + P\bar{A})e_d - 2e_d^T PK\alpha_1(x)Ce_d \\ &< -\delta e_d^T e_d - 2e_d^T C^T C\alpha_1(x)e_d \end{aligned}$$

where δ is a small positive scalar. Since the relative degree r from disturbance to output is uniformly well defined, it can be seen from (20) that $\alpha_1(x)$ regardless of x. As $e_d^T C^T C e_d > 0$, one can obtain that

$$V(e_d) < -\delta e_d^T e_d,$$

for any x and e. Thus it can be proven that that estimation $\hat{d}$ yielded by nonlinear disturbance observer can approach to disturbance d globally exponentially, and the convergence of disturbance observer regardless of x can be guaranteed by determining the gain K. □

The input to state stability of the closed-loop system can be proven by the following theorem.

Theorem 2. *The closed-loop system consists of nonlinear system, robust H_∞ control input and nonlinear disturbance observer is input to state stable if the following conditions are satisfied:*

1. The nonlinear model under the control input u is globally asymptotically stable in the nominal condition;

2. The vector-valued function $p(x)$ is chosen to make the observer error system be globally asymptotically stable.

Then there exist a disturbance observer compensation gain $\beta(x)$ such that:

$$m(x) + g(x)\beta(x) = G(\bar{x})M(\bar{x}), \tag{21}$$

where $G(\bar{x})$ and $M(\bar{x})$ are satisfied to

$$\dot{\bar{x}} = F(\bar{x}) + \begin{bmatrix} G(\bar{x})M(\bar{x}) & 0 \end{bmatrix}^T d,$$

It can be proven that the closed-loop system is input to state stability.

Proof. Combining the closed-loop system, the proposed control method, and disturbance error estimation, the nonlinear system can be rewritten as following expression:

$$\begin{aligned} \dot{x} &= [f(x) + g(x)\alpha(x)] - g(x)\beta(x)e + [m(x) + g(x)\beta(x)]e_d, \\ \dot{e} &= -\tfrac{\partial p(x)}{\partial x} m(x)e. \end{aligned} \tag{22}$$

Then the closed-loop system can be given as:

$$\dot{x} = F(\bar{x}) + \begin{bmatrix} m(x) + g(x)\beta(x) & 0 \end{bmatrix}^T e_d. \tag{23}$$

With the conditions given in 1 and 2, it can be seen that $\dot{\bar{x}} = F(\bar{x})$ is asymptotically stable in the nominal condition. Thus there exists a function $V(\bar{x})$ and a class κ_∞ function $R(\cdot)$ such that:

$$\forall(x) \in R^n/0 \Rightarrow \frac{\partial V}{\partial x} F(\bar{x}) < -R(\|x\|), \tag{24}$$

Considering the following system:

$$\dot{x} = H(\bar{x}, d) = F(\bar{x}) + \begin{bmatrix} G(\bar{x}) & 0 \end{bmatrix}^T e_d,$$

and combining the equation given as:

$$\forall(x) \in R^n/0 \Rightarrow \frac{\partial V}{\partial x} H(\bar{x}, 0) < -R(\|x\|),$$

It can be seen that there exists a matrix $M(\bar{x})$ which is nonsingular and defined for all x such that for some class function:

$$\forall\|x\| \geq \chi(\|d\|) \Rightarrow \frac{\partial V}{\partial x} H(\bar{x}, M(\bar{x})d) < -\frac{1}{2} R(\|x\|). \tag{25}$$

Consider the condition given in formal, then it can be concluded from (25) that the closed-loop system is input-to-state stability. □

Remark 5. From this section, the uncertainties including unmodeled nonlinearities, parametric uncertainties, and external disturbances are regard as the closed-loop system inputs. Then the closed-loop system is stable if the assumptions are satisfied and the disturbance compensation gain of the observer is bounded, from Theorem (1).

5. Simulation Results and Discussions

In this section, the experimental platform model is developed based on the "X-hound" aircraft. The tail-sitter aircraft is equipped with four Sunnysky motors. Each motor is able to provide a maximum thrust of $6.5N$ at a maximum rotor speed with GWS 8045 propeller. The length of the tail sitter from nose to tail is close to $0.9m$, and the wingspan is approximately $0.88m$. The overall weight of the aircraft is approximately $1.36kg$. The parameters of nominal aircraft model are shown as follows: $J_x = 0.083$, $J_{xy} = 2.077 \times 10^{-5}$, $J_y = 0.026$, $J_{yz} = -2.726 \times 10^{-4}$, $J_z = 0.101$, $J_{zx} = 4.707 \times 10^{-6}$, $\rho = 1.225$, $c = 1$, $S = 1$, $g_0 = 9.80665$, , $v_0 = 0$, $v_e = 15$ and $m = 1.36$. Some constant values of the system model are selected as follows: $c_1 = -0.937$,$c_2 = 9.029 \times 10^{-5}$, $c_3 = 12.501$, $c_4 = 5.825 \times 10^{-4}$, $c_5 = 0.808$, $c_6 = 1.810 \times 10^{-4}$, $c_7 = 38.461$, $c_8 = 0.534$, $c_9 = 9.901$, $\lambda_1 = 5.0 \times 10^{-4}$, $\lambda_2 = 3.0 \times 10^{-4}$, $l_1 = 0.25$, $l_2 = 0.2$, $l_3 = 0.305$, $l_4 = 0.2$. The aerodynamic coefficients values are selected as: $C_{X_0} = -2.2151$, $C_{X_1} = 0.0190$, $C_{Y_0} = 0$, $C_{Y_1} = -0.5861$, $C_{Z_0} = -3.1631$, $C_{Z_1} = -1.8390$, $C_{R_0} = -0.0261$, $C_{M_0} = 0.1763$, $C_{N_0} = 0$, $C_{R_1} = -0.0233$, $C_{M_1} = 0.0316$, $C_{N_1} = 0.0504$, $C_{R_2} = -0.0112$, $C_{M_2} = 0.0655$, and $C_{N_2} = 0.0146$.

In this article, the external disturbances are consisted of the sinusoidal periodic signals and the high frequency noise signals. Let $d_{ni}(i = 1, 2, 3, 4, 5, 6)$ represent the high frequency noise signals, and the values of the external disturbances can be given as follows: $d_{vx} =$

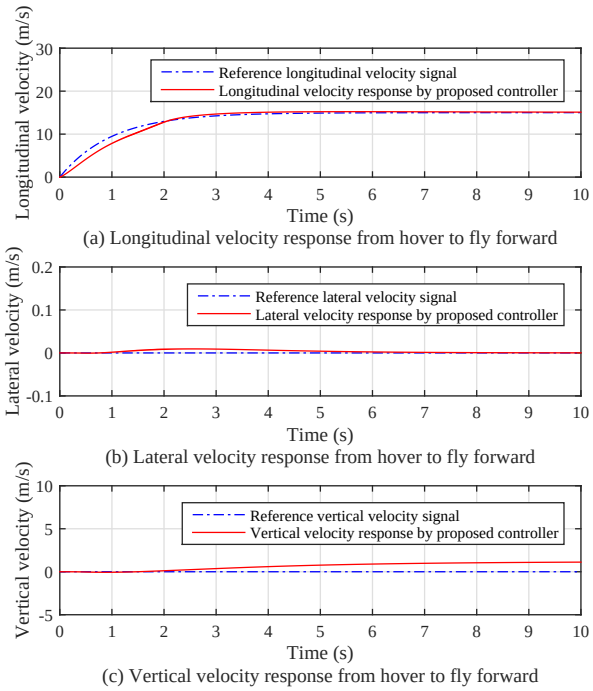

(a) Longitudinal velocity response from hover to fly forward

(b) Lateral velocity response from hover to fly forward

(c) Vertical velocity response from hover to fly forward

Fig. 4: Velocity responses for nominal model by proposed controller from hover to fly forward.

$0.5\sin(0.001\pi t) + d_{n1}$, $d_{vy} = 0.1\sin(0.001\pi t) + d_{n2}$, $d_{vz} = 0.1\sin(0.001\pi t) + d_{n3}$, $d_{\omega x} = 0.2\sin(0.001\pi t) + d_{n4}$, $d_{\omega y} = 0.2\sin(0.001\pi t) + d_{n5}$, and $d_{\omega z} = 0.2\sin(0.001\pi t) + d_{n6}$.

The proposed control law has been implemented on the simulation model to evaluate the performance of the closed-loop system. Two different cases would be simulated to evaluate the performance of the proposed controller on the mode transition from hover to fly forward and from fly forward to hover. To test the stability and tracking properties of the closed-loop control system, the nonlinear robust controller with disturbance observer discussed in this paper has been simulated. The aim of the proposed controller is to achieve the desired trajectory tracking and improve the robustness of the closed-loop system in transition conditions. The results of the proposed nonlinear robust controller have been shown to compare with the standard H_∞ controller to demonstrate the advantages of the proposed control method. Considering that the standard H_∞ controller may have the problem that the influence of the uncertainty cannot be suppressed in the whole frequency band, the standard H_∞ control method are introduced to be the nominal controller for achieving the tracking trajectory performance of the nominal system while the disturbance observer is designed to suppress the uncertainties. It is necessary to compare the current work with other methods in the literature. However, it is hard to tune the parameters of the control methods in the literature for optimal performances in simulation. Instead, the standard robust control method, i.e., H_∞ control method is compared to illustrate the advantages of our robust control method.

The final trajectory is established as the terminal constraint. During the transition flight, the process of the tail-sitter can consist of two phases: the hover-to-level flight and the level-to-hover. Let $\ddot{x}_b^r$, $\dot{x}_b^r$ and x_b^r represent the acceleration, velocity and position in the

level direction, while $\ddot{z}_b^r$, $\dot{z}_b^r$ and z_b^r represent the acceleration, velocity and position in the vertical direction.For a hover-to-level transition, the trajectory in the level direction can be given by

$$\ddot{x}_b^r = v_e a e^{-at},$$
$$\dot{x}_b^r = v_e(1 - e^{-at}) + v_0,$$
$$x_b^r = v_e(t + \tfrac{1}{a}e^{-at}) + v_0 t.$$

The desired trajectories in the vertical direction can be expressed as

$$\ddot{z}_b^r = h_0(1 - (k_r x_b^r)^2 e^{-k_r x_b^r}\dot{x}_b^r + k_r x_b^r e^{-k_r x_b^r}\ddot{x}_b^r),$$
$$\dot{z}_b^r = h_0(1 + k_r x_b^r e^{-k_r x_b^r}\dot{x}_b^r),$$
$$z_b^r = h_0(1 - e^{-k_r x_b^r}).$$

The trajectory in the pitch angle changes from 90° to 0° while the roll and yaw angle maintain at 0°. For level-to-hover transition, the trajectory in the level direction can be

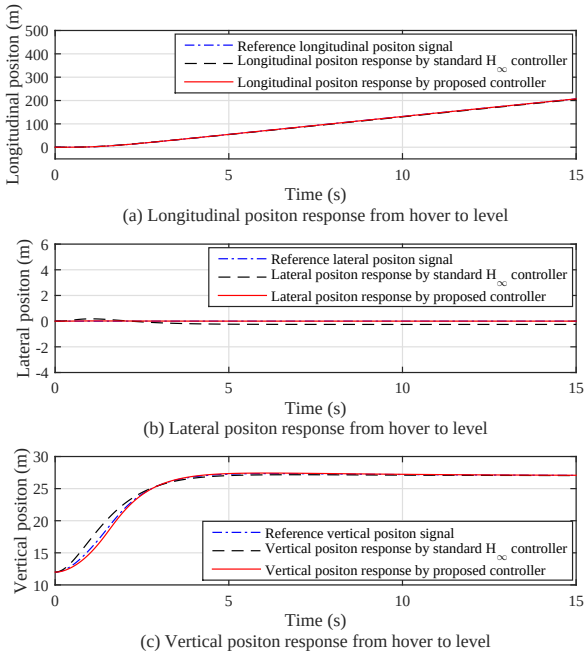

(a) Longitudinal positon response from hover to level

(b) Lateral positon response from hover to level

(c) Vertical positon response from hover to level

Fig. 5: Position responses for nominal model by proposed controller and standard H_∞ controller from hover to fly forward.

given by

$$\ddot{x}_b^r = -v_e a e^{-at},$$
$$\dot{x}_b^r = -v_e(1 - e^{-at}) + v_e,$$
$$x_b^r = -v_e(t + \tfrac{1}{a}e^{-at}) + v_e t.$$

The desired trajectories in the vertical direction can be expressed as

$$\ddot{z}_b^r = h_0(1 - (k_r x_b^r)^2 e^{-k_r x_b^r}\dot{x}_b^r + k_r x_b^r e^{-k_r x_b^r}\ddot{x}_b^r),$$
$$\dot{z}_b^r = h_0(1 + k_r x_b^r e^{-k_r x_b^r}\dot{x}_b^r),$$
$$z_b^r = h_0(1 - e^{-k_r x_b^r}).$$

As the tail-sitter aircraft assumes a hover position, the pitch angle should changes from zero to the vertical angle, the roll and yaw angles maintain at 0°.The related parameters are selected as $a = 1$, $k_r = 0.5$, $v_e = 15m/s$, $v_0 = 0m/s$, and $h_0 = 12m$.

Simulations of a standard H_∞ controller and the proposed robust controller have been conducted for the nominal model and uncertain nonlinear model, respectively.From the following simulation results, it can be observed that the proposed robust nonlinear control method improve the tracking performance and robustness of the closed-loop control system. By the standard H_∞ controller, the influence of uncertainties cannot be restrained in the whole frequency range; but the proposed robust nonlinear control methodology, can reduced the influences of uncertainties as small as desired by the nonlinear disturbance observer. Thus the tracking performance and robustness are improved, compared with the standard H_∞ method. A similar results can be seen in [40], a transient process cost approximate 20 seconds for the pitch angle and thereby. It can be shown that the standard H_∞ controller cannot specify the transient tracking performance.

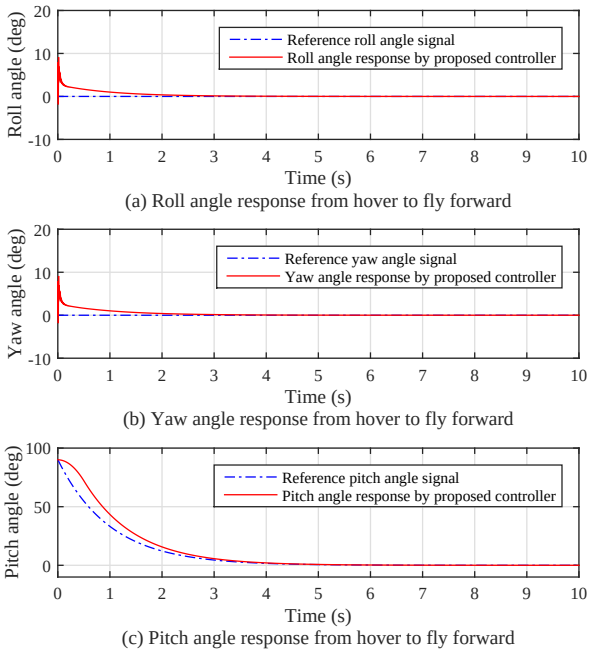

(a) Roll angle response from hover to fly forward

(b) Yaw angle response from hover to fly forward

(c) Pitch angle response from hover to fly forward

Fig. 6: Attitude responses for nominal model by proposed controller from hover to fly forward.

Case 1: In this simulation, the two transition flights are based on the nominal model. The results of the proposed robust control method and standard H_∞ control method are given. In the nominal model neglected the parameter uncertainties and the external disturbance, it can be seen from Fig. 4, Fig. 5, Fig. 6, Fig. 7, Fig. 8, Fig. 9, Fig. 10, and Fig. 11 that both the robust controller with disturbance observer and the standard H_∞ controller can achieve the reference command tracking control, while the proposed controller can achieve the desired trajectory tracking with less time.

Case 2: In this simulation, the two transition flights are based on the nonlinear model with the uncertainties and disturbances. The results of the proposed robust control method

and standard H_∞ control method are given. With the parameter uncertainties and the external disturbance, it can be seen from Fig. 12, Fig. 13, Fig. 14, Fig. 15, Fig. 16, Fig. 17, Fig. 18 and Fig. 19 that the robust controller with disturbance observer can achieve the reference command tracking control better than the standard H_∞ controller under the influence of uncertainties.

From these figures, it can be found that the proposed closed-loop control system can achieve good tracking performance and steady-state performance. It can be observed that the proposed robust nonlinear control method improve the tracking performance and robustness of the closed-loop control system and prevent longitudinal maneuvering from affecting lateral motion.The desired trajectory tracking control can be achieved under the influence of uncertainties including unmodeled nonlinearities, parametric uncertainties, and external disturbances. It can be observed that the tail-sitter aircraft can address the mode transition from hover to fly forward with small velocity and attitude errors in the whole process. Therefore, the proposed controller can achieve the desired trajectory tracking and improve the robustness of the closed-loop system.

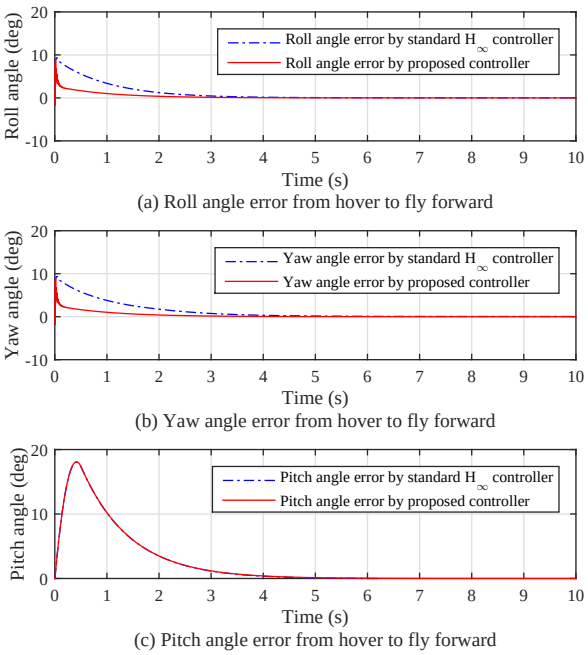

(a) Roll angle error from hover to fly forward

(b) Yaw angle error from hover to fly forward

(c) Pitch angle error from hover to fly forward

Fig. 7: Attitude error for nominal model between proposed controller and standard H_∞ controller from hover to fly forward.

6. CONCLUSIONS

This paper has presented a robust H_∞ controller with nonlinear disturbance observer for the tail-sitter aircraft to deal with the trajectory tracking control problem of mode transition. The nonlinear model with uncertainties is simplified and the nominal model is obtained. The linear time-invariant H_∞ controller is designed in nominal condition and

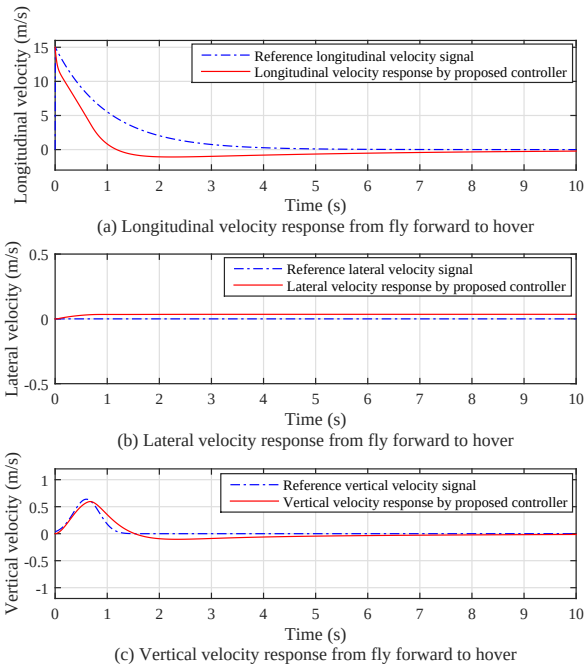

(a) Longitudinal velocity response from fly forward to hover

(b) Lateral velocity response from fly forward to hover

(c) Vertical velocity response from fly forward to hover

Fig. 8: Velocity responses for nominal model by proposed controller from fly forward to hover.

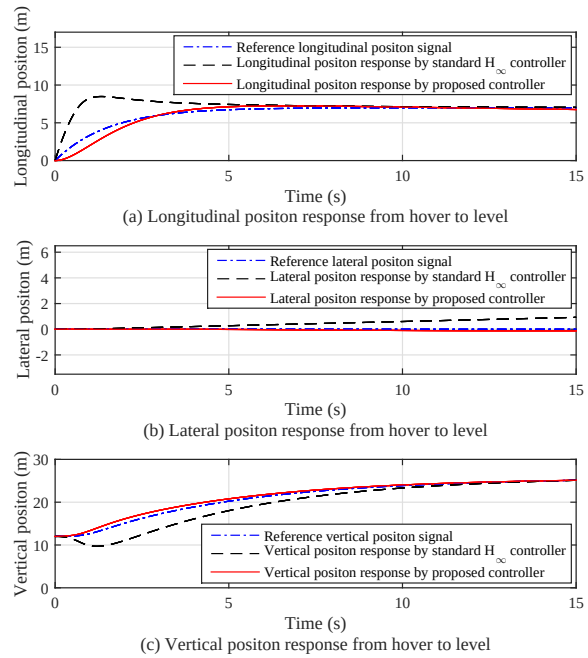

(a) Longitudinal positon response from hover to level

(b) Lateral positon response from hover to level

(c) Vertical positon response from hover to level

Fig. 9: Positon responses for nominal model by proposed controller and standard H_∞ controller from fly forward to hover.

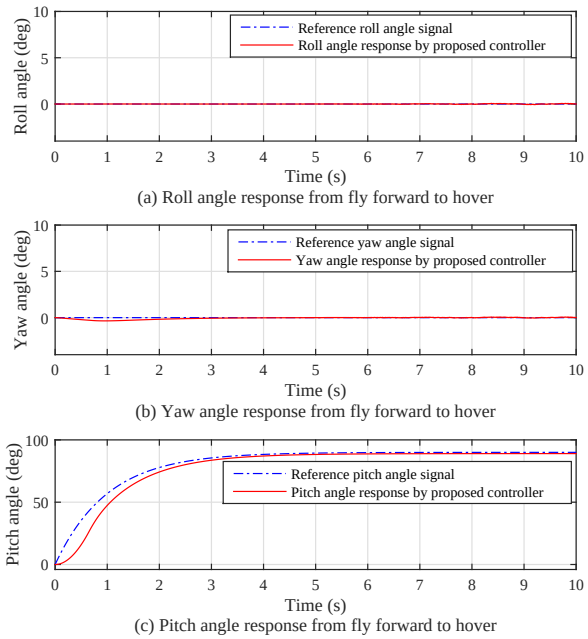

(a) Roll angle response from fly forward to hover

(b) Yaw angle response from fly forward to hover

(c) Pitch angle response from fly forward to hover

Fig. 10: Attitude responses for nominal model by proposed controller from fly forward to hover.

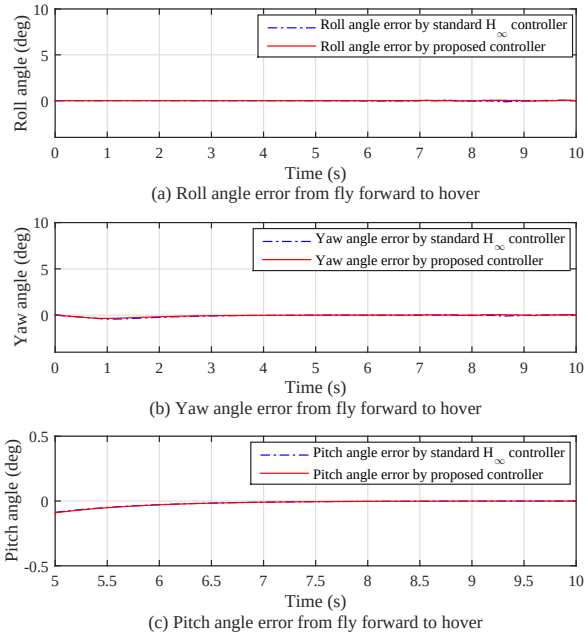

(a) Roll angle error from fly forward to hover

(b) Yaw angle error from fly forward to hover

(c) Pitch angle error from fly forward to hover

Fig. 11: Attitude error for nominal model between proposed controller and standard H_∞ controller from fly forward to hover.

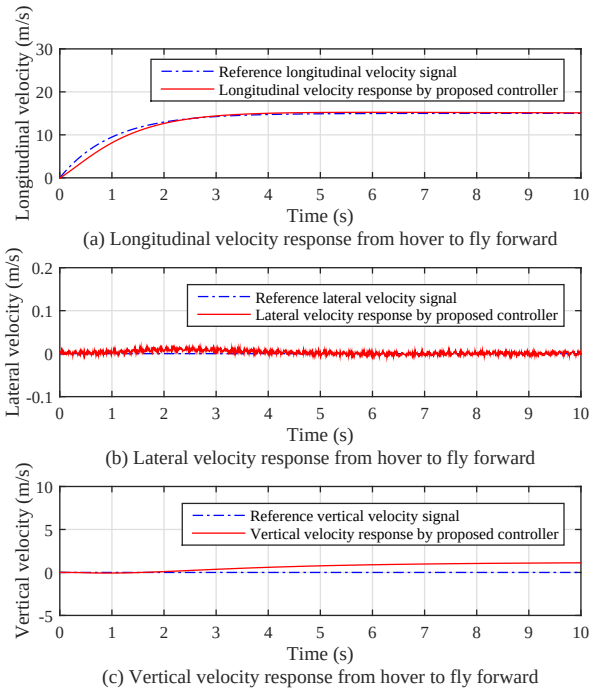

(a) Longitudinal velocity response from hover to fly forward

(b) Lateral velocity response from hover to fly forward

(c) Vertical velocity response from hover to fly forward

Fig. 12: Velocity responses under uncertainties by proposed controller from hover to fly forward.

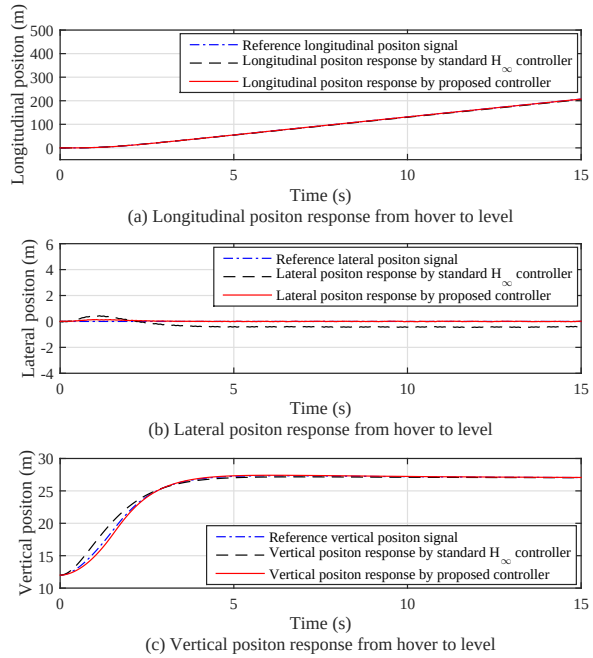

(a) Longitudinal positon response from hover to level

(b) Lateral positon response from hover to level

(c) Vertical positon response from hover to level

Fig. 13: Position responses under uncertainties by proposed controller and standard H_∞ controller from hover to fly forward.

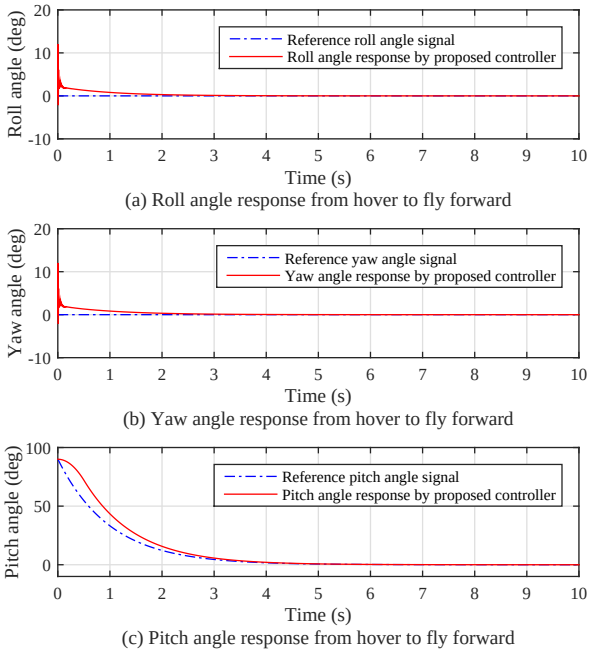

(a) Roll angle response from hover to fly forward

(b) Yaw angle response from hover to fly forward

(c) Pitch angle response from hover to fly forward

Fig. 14: Attitude responses under uncertainties by proposed controller from hover to fly forward.

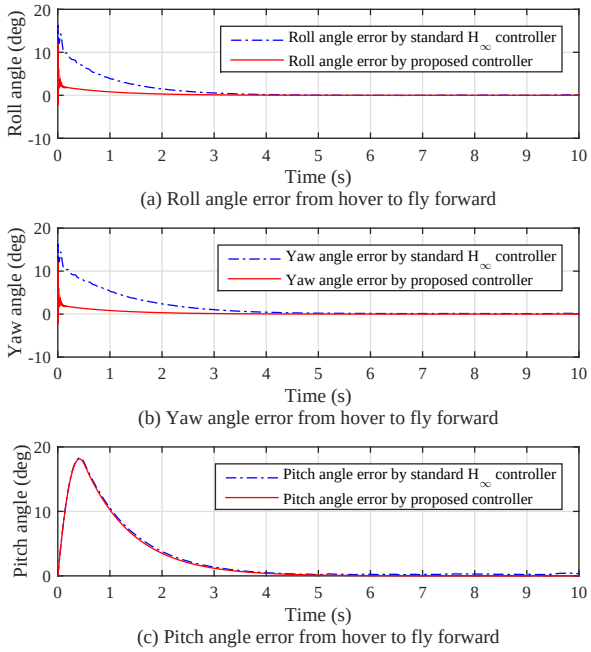

(a) Roll angle error from hover to fly forward

(b) Yaw angle error from hover to fly forward

(c) Pitch angle error from hover to fly forward

Fig. 15: Attitude error under uncertainties between proposed controller and standard H_∞ controller from hover to fly forward.

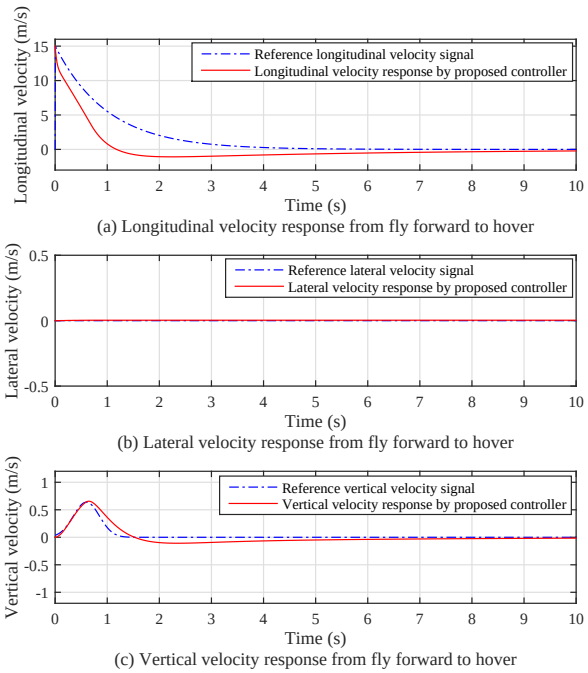

(a) Longitudinal velocity response from fly forward to hover

(b) Lateral velocity response from fly forward to hover

(c) Vertical velocity response from fly forward to hover

Fig. 16: Velocity responses under uncertainties by proposed controller from fly forward to hover.

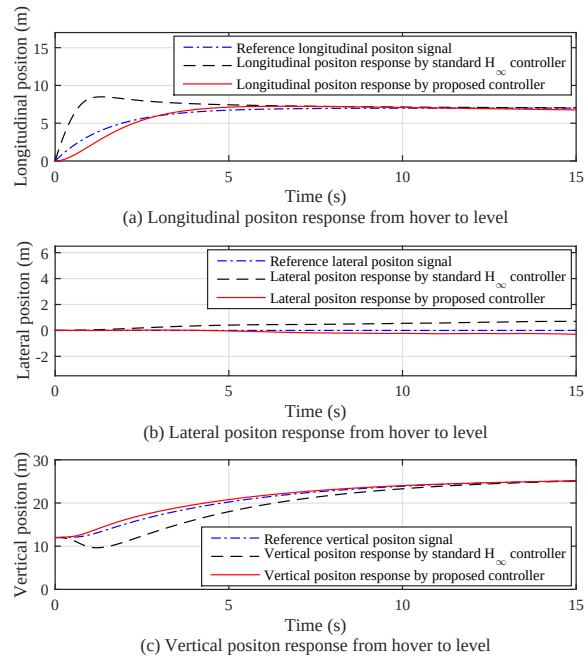

(a) Longitudinal positon response from hover to level

(b) Lateral positon response from hover to level

(c) Vertical positon response from hover to level

Fig. 17: Position responses under uncertainties by proposed controller and standard H_∞ controller from fly forward to hover.

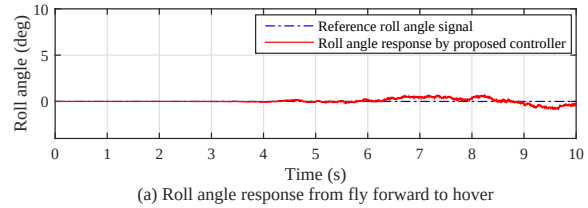

(a) Roll angle response from fly forward to hover

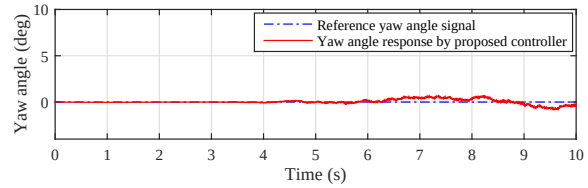

(b) Yaw angle response from fly forward to hover

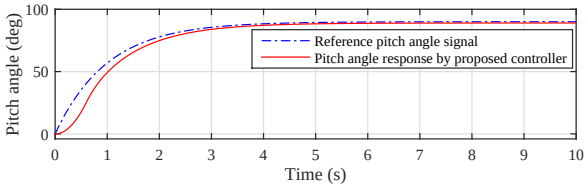

(c) Pitch angle response from fly forward to hover

Fig. 18: Attitude responses under uncertainties by proposed controller from fly forward to hover.

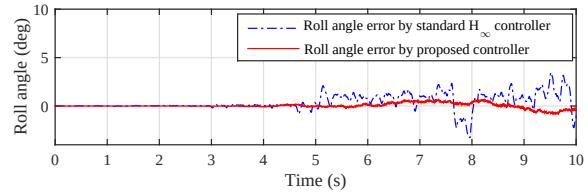

(a) Roll angle error from fly forward to hover

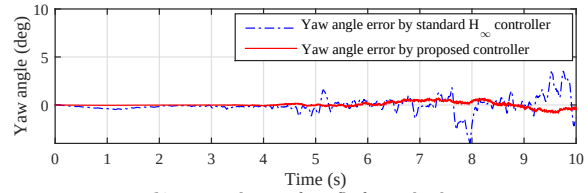

(b) Yaw angle error from fly forward to hover

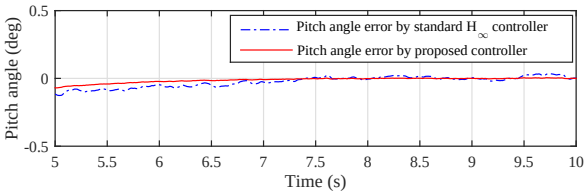

(c) Pitch angle error from fly forward to hover

Fig. 19: Attitude error under uncertainties between proposed controller and standard H_∞ controller from fly forward to hover.

the disturbance observer is introduced based on the nonlinear model. It is proved that the closed-loop system is stable, and the tracking error can converge to near the small neighborhood. It is shown that the proposed robust controller with disturbance observer can maintain the adjustment accuracy and robustness to the model external disturbance.

Acknowledgements

This work was supported by the National Natural Science Foundation of China under Grants 61503012 and 61673034, and the Fundamental Research Funds for the Central Universities under Grants YWF-18-BJ-Y-81 and YWF-17-BJ-Y-86.

References

[1] B. Herisse, T. Hamel, R. Mahony, and F. Russotto, Landing a VTOL unmanned aerial vehicle on a moving platform using optical flow, *IEEE Transactions on Robotics*, vol. 28, no. 1, pp. 77-89, 2012.

[2] H. Du, W. Zhu, G. Wen, and D. Wu, Finite-time formation control for a group of quadrotor aircraft, *Aerospace Science and Technology*, vol. 69, no. 1, pp. 609-616, 2017.

[3] A. Oosedo, S. Abiko, A. Konno, and M. Uchiyama, Optimal transition from hovering to level-flight of a quadrotor tail-sitter UAV, *Autonomous Robots*, vol. 41, no. 5, pp. 1143-1159, 2017.

[4] M. Radmanesh and M. Kumar Flight formation of UAVs in presence of moving obstacles using fast-dynamic mixed integer linear programming, *Aerospace Science and Technology*, vol. 50, no. 1, pp. 149-160, 2016.

[5] M. A. Dehghani and M. B. Menhaj, Integral sliding mode formation control of fixed-wing unmanned aircraft using seeker as a relative measurement system, *Aerospace Science and Technology*, vol. 58, no. 1, pp. 318-327, 2016.

[6] A. Banazadeh and N. Taymourtash, Optimal control of an aerial tail sitter in transition flight phases, *Journal of Aircraft*, vol. 53, no. 4, pp. 914-921, 2016.

[7] A. Ailon, Simple tracking controllers for autonomous VTOL aircraft with bounded inputs, *IEEE Transactions on Automatic Control*, vol. 55, no. 3, pp. 737-743, 2010.

[8] B. Wang, Z. Hou, and Z. Guo, Space range estimate for battery-powered vertical take-off and landing aircraft, *Journal of Central South University*, vol. 22, no. 9, pp. 3338-3346, 2015.

[9] K. Adam, D. Ludovic, and B. Adrien, An active uprighting mechanism for flying robots, *IEEE Transactions on Robotics*, vol. 28, no. 5, pp. 1152-1157, 2012.

[10] J. L. Forshaw and V. J. Lappas, Architecture and systems design of a reusable Martian twin rotor tailsitter, *Acta Astronautica*, vol. 80, pp. 166-180, 2012.

[11] J. L. Forshaw, V. J. Lappas, and P. Briggs, Transitional control architecture and methodology for a twin rotor tailsitter, *Journal of Guidance Control and Dynamics*, vol. 37, no.4, pp. 1289-1298, 2014.

[12] X. Wang, Z. Chen, and Z. Yuan, Modeling and control of an agile tail-sitter aircraft, *Journal of the Franklin Institute*, vol. 352, no. 12, pp. 5437-5472, 2015.

[13] K. Wang, Y. Ke, and B. M. Chen, Autonomous reconfigurable hybrid tail-sitter UAV U-Lion, *Science China Information Sciences*, vol. 60, no. 3, 2016.

[14] H. Li, C. Li, H. Li, Y. Li, and Z. Xing, An integrated altitude control design for a tail-sitter UAV equipped with turbine engines, *IEEE Access*, vol. 5, pp. 10941-10952, 2017.
[15] L. Fu, L. Wang, and X. Yang, Development of a rotorcraft micro air vehicle for indoor flight research, *Journal of Intelligent and Robotic Systems*, vol. 81, no. 3-4, pp. 423-441, 2016.
[16] K. Chinwicharnam, E. Ariza, J. Moschetta, and C. Thipyopas, A computation study on the aerodynamic influence of interaction wing-propeller for a tilt-body MAV, *Aircraft Engineering and Aerospace Technology*, vol. 87, no. 6, pp. 521-529, 2015.
[17] F. Lin, W. Zhang, R. Brandt, Robust hovering control of a PVTOL aircraft, *IEEE Transactions on Control Systems and Technology*, vol. 7, no. 3, pp. 343-351, 1999.
[18] D. Song, J. Han, and G. Liu, Active model-Based predictive control and experimental investigation on unmanned helicopters in full flight envelope, *IEEE Transactions on Control Systems Technology*, vol. 21, no. 4, pp. 1502-1509, 2013.
[19] I. A. Raptis,K. P. Valavanis, and G. J. Vachtsevanos, Linear tracking control for small-scale unmanned helicopters, *IEEE Transactions on Control Systems Technology*, vol. 20, no. 4, pp. 995-1010, 2012.
[20] T. Ryan and H. J. Kim, LMI-based gain synthesis for simple robust quadrotor control, *IEEE Transactions on Automation Science and Engineering*, vol. 10, no. 4, pp. 1173-1181, 2013.
[21] H. Du, W. zhu, G. Wen, Z. Duan, and J. Lv, Distributed formation control of multiple quadrotor aircraft based on non-smooth consensus algorithms, *IEEE Transactions on Cybernetics*, pp. 2168-2267, 2017.
[22] H. Du, and S. Li, Attitude synchronization for flexible spacecraft with communication delays, *IEEE Transactions on Automatic Control*, vol. 61, no. 11, pp. 3625-3630, 2017.
[23] T. Lee, Robust adaptive attitude tracking on SO(3) with an application to a quadrotor UAV, *IEEE Transactions on Control Systems Technology*, vol. 21, no. 5, pp. 1924-1930, 2013.
[24] R. Naldi, M. Furci, R. G. Sanfellice, and L. Marconi, Robust global trajectory tracking for underactuated VTOL aerial vehicles using inner-outer loop control paradigms, *IEEE Transactions on Automatic Control*, vol. 62, no. 1, pp. 97-112, 2017.
[25] H. Liu, J. Xi, and Y. Zhong, Robust attitude stabilization for nonlinear quadrotor systems with uncertainties and delays, *IEEE Transactions on Industrial Electronics*, vol. 64, no. 7, pp. 5585-5594, 2017.
[26] M. Lopez-Martinez, M. G. Ortega, C. Vivas, and F. R. Rubio, Nonlinear L2 control of a laboratory helicopter with variable speed rotors, *Automatica*, vol. 43, no. 4, pp. 655-661, 2007.
[27] B. Zhao, B. Xian, Y. Zhang, and X. Zhang, Nonlinear robust adaptive tracking control of a quadrotor UAV via immersion and invariance methodology, *IEEE Transactions on Industrial Electronics*, vol. 62, no. 5, 2015.
[28] H. Liu, W. Zhao, Z. Zuo, and Y. Zhong, Robust control for quadrotors with multiple time-varying uncertainties and delays, *IEEE Transactions on Industrial Electronics*, vol. 64, no. 2, pp. 1303-1312, 2017.
[29] H. Liu, D. Li, Z. Zuo, and Y. Zhong, Robust three-loop trajectory tracking control for quadrotors with multiple uncertainties, *IEEE Transactions on Industrial Electronics*,

vol. 63, no. 4, pp. 2263-2274, 2016.
[30] F. Chen, F. Lu, B. Jiang, and G. Tao Adaptive compensation control of the quadrotor helicopter using quantum information technology and disturbance observer, *Journal of the Franklin Institute*, vol. 351, no. 1, pp. 442-455, 2014.
[31] J. She, M. Fang, Y. Ohyama, and H. Hashimoto, Improving disturbance-rejection performance based on an equivalent-input-disturbance approach, *IEEE Transactions on Industrial Electronics*, vol. 55, no. 1, pp. 380-389, 2008.
[32] L. Wang and J. Su, Robust disturbance rejection control for attitude tracking of an aircraft, *IEEE Transactions on Control Systems Technology*, vol. 23, no. 6, pp. 2361-2368, 2015.
[33] H. Menno, N. Cyriel, and T. Bart, Design and control of an unmanned aerial vehicle for autonomous parcel delivery with transition from vertical take-off to forward flight, *International Journal of Micro Air Vehicles*, vol. 7, no. 4, pp. 395-405, 2015.
[34] A. Mirac and I. Gokhan, Design methodology of a hybrid propulsion driven electric powered miniature tailsitter unmanned aerial vehicle, *Journal of Intelligent and Robotic Systems*, vol. 57, no. 1-4, pp. 505-529, 2010.
[35] W. Hu and J. Zhou, Design of neural network variable structure reentry control system for reusable launch vehicle, *Journal of China Ordnance*, vol. 4, no. 3, pp. 191-197, 2008.
[36] M. A. Bolender and D. B. Doman, Nonlinear control allocation using piecewise linear functions, *Journal of Guidance Control and Dynamics*, vol. 27, no. 6, pp. 1017-1027, 2004.
[37] G. Cai, B. M. Chen, X. Dong, and T. H. Lee, Design and implementation of a robust and nonlinear flight control system for an unmanned helicopter, *Mechatronics*, vol. 21, pp. 803-820, 2011.
[38] W. Chen, D. J. Ballance, P. J. Gawthrop, and J. O. Reilly, A nonlinear disturbance observer for robotic manipulators, *IEEE Transactions on Industrial Electronics,*, vol. 47, no. 4, pp. 932-938, 2000.
[39] C. Liu, W. Chen, and J. Andrews, Tracking control of small-scale helicopters using explicit nonlinear MPC augmented with disturbance observers, *Control Engineering Practice*, vol. 20, pp. 258-268, 2012.
[40] B. Zhao, B. Xian, Y. Zhang, and X. Zhang, Nonlinear robust sliding mode control of a quadrotor unmanned aerial vehicle based on immersion and invariance method, *International Journal of Robust and Nonlinear Control*, vol. 25, no. 18, pp. 3714-3731, 2015.